

## Stepwise Electron–Laser Excitation Studies of Atoms

*C. W. McLucas, W. R. MacGillivray and M. C. Standage*

School of Science, Griffith University, Nathan, Qld 4111.

### *Abstract*

A new stepwise excitation technique is presented in which single-mode laser excitation is used to probe isotopic effects in inelastic scattering processes between electrons and mercury atoms.

### 1. Introduction

The application of lasers to the field of electron collisions with atoms and molecules has led to the development of a range of techniques which yield new information about collision processes. Dye lasers tuned to selected atomic and molecular transitions can produce substantial excited state populations which allow the super-elastic scattering of electrons from atoms and molecules to be studied (Hertel and Stoll 1977; Register *et al.* 1978). Such measurements provide an alternative method to electron–photon coincidence techniques for measuring not only the magnitude but also the relative phase of electron excitation amplitudes.

Cross-section measurements on laser excited atoms have been performed using the photon recoil effect caused by intense resonant laser excitation, which physically deflects a highly collimated atomic beam (Bhaskar *et al.* 1976). Several stepwise excitation techniques have been recently developed which involve electron and laser excitation. The excited state structure of atomic negative ion states has been investigated with stepwise electron and pulsed laser excitation (Langendam *et al.* 1976). Metastable atomic states have been studied using electron and multi-mode c.w. laser excitation (Phillips *et al.* 1981).

In this paper we present a theoretical and experimental discussion of a new application of stepwise excitation techniques to atomic collision studies. Atoms are excited by a combination of electron and single-mode laser excitation. Fluorescence emitted from the stepwise excited atoms is then measured for intensity and polarization as a function of the incident electron energy. Such measurements allow the excitation cross section and the line polarization of the electron impact excited transition to be determined. This technique allows several aspects of atomic collision physics to be studied in new detail. The narrow bandwidth of the laser radiation permits the fine and hyperfine structure of many atoms to be resolved in the laser excitation transition, allowing the roles of spin–orbit coupling and nuclear spin to be studied in electron–atom collisions. In suitable cases, the validity of the Percival–Seaton (1957) hypothesis that the nuclear spin plays no role in the collision process may be tested. Stepwise

excitation techniques of this type also offer a new method for obtaining line polarization measurements of electron impact excited VUV transitions and for studying electron excitation of metastable states and highly excited states.

The feasibility of using this stepwise excitation method was investigated by studying stepwise excitation schemes for the  $I = 0$  and  $\frac{1}{2}$  isotopes of mercury in which the  $6^1S_0-6^1P_1$  (185 nm) transition is excited by electron impact followed by single-mode laser excitation of the  $6^1P_1-6^1D_2$  (579 nm) transition (see Fig. 1). The hyperfine structure of the latter transition is well resolved compared with the Doppler width of the atomic beam used in this experiment, allowing laser excitation of different mercury isotopes. Measurements of the intensity and polarization of fluorescence emitted from the  $6^1D_2-6^3P_1$  (313 nm) transition allowed the excitation cross section and the line polarization of the electron impact excited transition to be determined for different isotopes. Further details of this work are contained in McLucas *et al.* (1982*a*, 1982*b*).

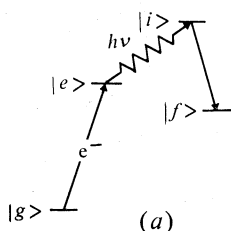
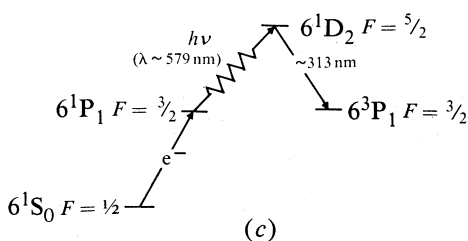
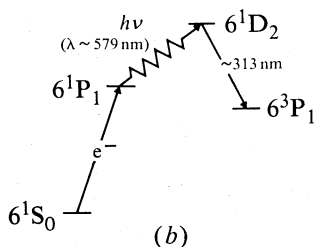


Fig. 1. Stepwise excitation:  
(a) General scheme.  
(b)  $I = 0$  scheme.  
(c)  $I = \frac{1}{2}$  scheme used in the experiment.



## 2. Theory

A theoretical expression for the fluorescence intensity emitted following the stepwise excitation of a single atom is given by McLucas *et al.* (1982*b*):

$$I = C \sum_{mm'uu'} A_{m'm} E_{uu'} F_{u'u} \int_0^{\delta t} \exp\{-\Gamma + i(w_{mu} - w_{m'u'})\} t dt, \quad (1)$$

where  $\Gamma$  is the decay constant associated with the fluorescence emission step, the terms  $w_{mu} - w_{m'u'}$  give the sublevel splittings for the laser excited transition,  $C$  is a geometrical factor and  $\delta t$  is the observation time of the detector. It has been assumed that both the electron and laser excitation steps take place in a time short compared with  $\Gamma$ . In equation (1),  $A$  and  $E$  are excitation operators which describe the electron and laser excitation processes respectively, while  $F$  is an emission operator representing the fluorescence emission of the stepwise excited atom. In the limit of weak laser

excitation, for which no significant optical pumping of the laser excited transition occurs, it can be shown that (McLucas *et al.* 1982*b*)

$$E_{uu'} = \langle u | e \cdot P | m \rangle \langle m' | e^* \cdot P | u' \rangle, \quad (2a)$$

$$F_{u'u} = \sum_n \langle u' | f \cdot P | n \rangle \langle n | f^* \cdot P | u \rangle, \quad (2b)$$

where  $|m\rangle$ ,  $|u\rangle$  and  $|n\rangle$  are magnetic sublevels of states  $|e\rangle$ ,  $|i\rangle$  and  $|f\rangle$  (see Fig. 1*a*),  $e$  and  $f$  are the polarization vectors of the laser field and scattered fluorescence respectively, and  $P$  is the electric dipole moment operator. An expression for the intensity emitted from an ensemble of stepwise excited atoms may be obtained by assuming cylindrical symmetry about the electron beam direction. In this case only the diagonal terms of the electron excitation matrix elements  $A_{m'm}$  are non-zero, and  $A_{11} = A_{-1-1}$ . In the notation of Macek and Jaecks (1971)  $A_{mm} = \langle a_m a_m \rangle$ , where  $a_m$  is the amplitude for electron excitation from the ground state to the  $m$ th sublevel of the first excited state, which may be written as

$$|e(t=0)\rangle = a_1 |1\rangle + a_0 |0\rangle + a_{-1} |-1\rangle. \quad (3)$$

Integration of  $A_{mm}$  over the electron scattering angles yields the partial integral cross sections  $Q_m$ .

For the  $I = 0$  stepwise  $6^1S_0 \rightarrow 6^1P_1 \rightarrow 6^1D_2 \rightarrow 6^3P_1$  transition of mercury studied in this work (see Fig. 1*b*), with the excitation and emission operator matrix elements evaluated for the experimental geometry shown in Fig. 2 and with circularly polarized laser excitation, we obtain from equations (1) and (2)

$$I(\beta) \propto 9Q_0(1 + \cos^2\beta) + Q_1(38 - 30\cos^2\beta), \quad (4)$$

where  $\beta$  is the angle the linear polarizer makes with the electron beam direction. The 313 nm line polarization is given by

$$P'_0 = \frac{I(0^\circ) - I(90^\circ)}{I(0^\circ) + I(90^\circ)} = \frac{9Q_0/Q_1 - 30}{27Q_0/Q_1 + 46}. \quad (5)$$

The electron impact excited 185 nm line polarization is given by

$$P_0 = \frac{Q_0/Q_1 - 1}{Q_0/Q_1 + 1}, \quad (6)$$

where the ratio  $Q_0/Q_1$  is obtained from equation (5).

The corresponding expression for the  $I = \frac{1}{2}$  isotope can be obtained in the following way. If we assume that the Percival-Seaton (1958) hypothesis holds during the collision process (i.e. the nuclear spin quantum numbers  $I$  and  $M_I$  remain unchanged), the first excited state  $6^1P_1$  with  $F = \frac{3}{2}$  (see Fig. 1*c*) can be expressed in terms of the  $I = 0$  excitation amplitudes as (McLucas *et al.* 1982*b*)

$$|e(t=0)\rangle = a_1 |\frac{3}{2}\rangle + (\sqrt{\frac{2}{3}} a_0 + \sqrt{\frac{1}{3}} a_1) |\frac{1}{2}\rangle + (\sqrt{\frac{2}{3}} a_0 + \sqrt{\frac{1}{3}} a_{-1}) |-\frac{1}{2}\rangle + a_{-1} |-\frac{3}{2}\rangle. \quad (7)$$

The hyperfine sublevel excitation amplitudes of equation (7) are used to construct electron excitation matrix elements, and the resultant expression for the fluorescence intensity emitted from the stepwise excited  $6^1D_2$   $F = \frac{5}{2}$  state for  $I = \frac{1}{2}$  is given by

$$I(\beta) \propto Q_0(3\cos^2\beta + 4) + Q_1(10\sin^2\beta + 5). \quad (8)$$

The corresponding 313 nm line polarization for the  $I = \frac{1}{2}$  isotope is given by

$$P'_{\frac{1}{2}} = \frac{3Q_0/Q_1 - 10}{11Q_0/Q_1 + 20}. \quad (9)$$

Equations (8) and (9) are valid only if the Percival–Seaton hypothesis holds. Under this hypothesis the 185 nm line ( $I = \frac{1}{2}$ ) polarization is given by (McConnell and Moiseiwitsch 1968)

$$P_{\frac{1}{2}} = \frac{3(Q_0/Q_1 - 1)}{7Q_0/Q_1 + 11}. \quad (10)$$

For heavy atoms such as mercury, spin-orbit interactions and the breakdown of  $LS$  coupling can play a significant role in the scattering process. However, the predominantly singlet character of the  $6^1P_1$  state, which only has a small admixture of the  $6^3P_1$  state, minimizes the effect of spin-orbit interactions in the electron excitation process. It has also been shown recently that the breakdown of  $LS$  coupling affects only the off-diagonal elements of the electron excitation operator (Blum *et al.* 1980) and hence does not alter equation (1). It can also be shown (McLucas *et al.* 1982*b*) that the breakdown in  $LS$  coupling does not change the polarization of the fluorescence emitted following the stepwise excitation.

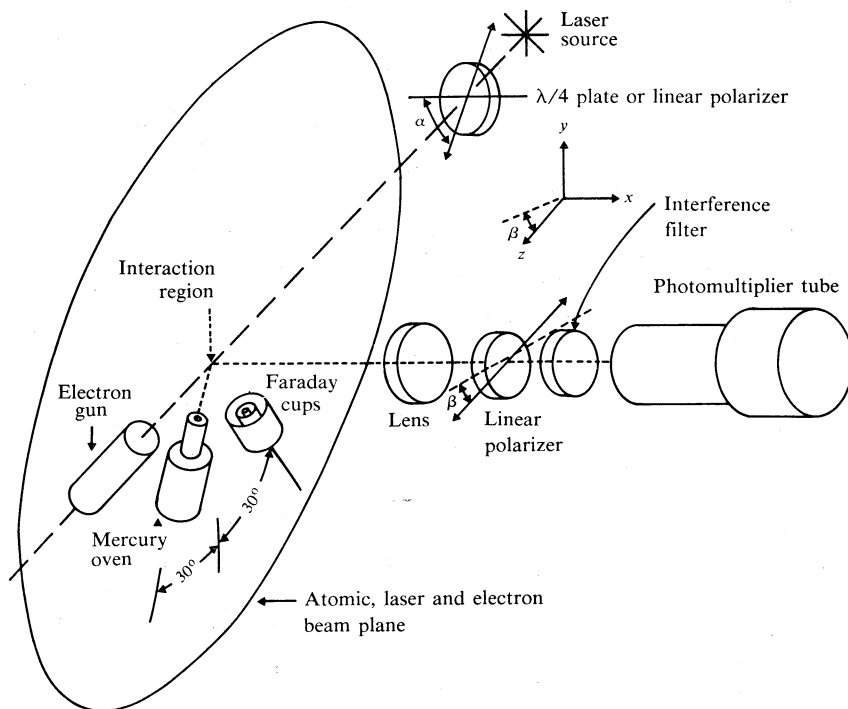
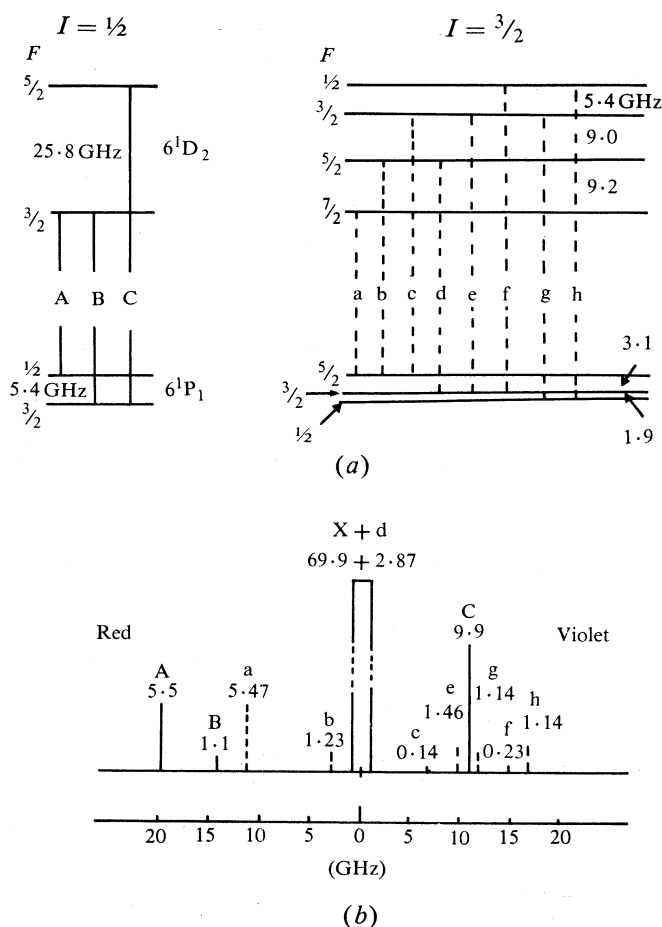


Fig. 2. Geometrical arrangement of the experiment (see text).

### 3. Experiment

A schematic diagram of the experiment is shown in Fig. 2. A turntable system mounted off an end flange of the vacuum system carried the electron gun, Faraday cups and the atomic beam source. Most components including the vacuum chamber

were fabricated from non-magnetic stainless steel. A set of Helmholtz coils placed around the vacuum chamber cancelled the Earth's magnetic field. The laser beam was sent through an optical window and intersected the electron and atomic beam. Fluorescence scattered from the interaction region was collected by a quartz lens and focussed through another optical window onto a photon detection system mounted on the end flange of the vacuum system opposite to the turntable system. This system consisted of a UV linear polarizer, a 313 nm interference filter and a Philips 150 AVP photomultiplier tube cooled by Peltier coolers. The effective solid angle of the detector was  $2 \times 10^{-2}$  sr. The photon count rate was recorded as a function of the polarizer angle using standard photon counting equipment.



**Fig. 3.** In (a) the hyperfine splittings for the  $6^1P_1$  and  $6^1D_2$  levels in the  $I = 1/2$  (left) and  $I = 3/2$  (right) nuclear spin isotopes of mercury are shown. In (b) the relative intensities and spectral positions of these hyperfine transitions are given.

An electron gun of the electrostatic aperture lens type was used. The electron source was a heated tungsten hair-pin filament. Electrons were accelerated and focussed by a two stage system consisting of a two aperture lens followed by a three aperture 'zoom' lens. The gun was designed to operate in the 5–20 eV energy range

with currents of 1–5  $\mu\text{A}$ . A system of three concentric Faraday cups of diameters 2, 5 and 10 mm were used to tune the electron gun as well as determine the beam profile. The Faraday cups could be moved in and out of the interaction region on a screw driven slide operated by a rotary motion feedthrough.

The atomic beam was produced by effusing mercury vapour from a heated non-magnetic stainless steel oven. The oven consisted of two sections, each independently heated, so that the top section could be operated at about 20°C above the bottom section to prevent clogging of the output nozzle. A liquid nitrogen cooled plate was used to trap the mercury after it had traversed the interaction region. The collimation factor of about 3 : 1 was determined by measuring the diameter of the mercury spot deposited on the plate. Under normal operating conditions, the pressure in the oven was estimated to be about 0.5 Torr (= 66 Pa), giving an atomic beam density in the interaction region of approximately  $10^{13}$  atoms  $\text{cm}^{-3}$ . An oil diffusion pump (Edwards Diffstak 160/170) maintained a background operating pressure of  $(3\text{--}5) \times 10^{-6}$  Torr for the  $I = 0$  runs and gave an ultimate pressure of approximately  $10^{-7}$  Torr.

Laser radiation was provided by a Spectra-Physics 380 A single-mode ring dye laser. A small fraction of the laser light was sent through a Philips mercury spectral lamp which was used as a frequency reference. When the laser was tuned, strong absorption occurred due to stepwise excitation in the lamp. Fig. 3a illustrates the hyperfine splittings for the  $6^1\text{P}_1 \rightarrow 6^1\text{D}_2$  transition in the  $\frac{1}{2}$  (*left*) and  $\frac{3}{2}$  (*right*) spin isotopes, while Fig. 3b shows the relative positions of all the hyperfine transitions together with their relative intensities (Schüler and Jones 1932). No difficulty was encountered in detecting the transitions X, A, a and C in the spectral lamp.

The total fluorescence recorded by the photon detector consists in general of a signal due to direct electron excitation of the  $^1\text{D}_2$ ,  $^3\text{D}_1$  and  $^3\text{D}_2$  levels as well as the stepwise excited signal. The relative strength of the stepwise to direct signal was typically 50% at 9 eV and increased at lower energies as the direct signal diminished. Measurements at a particular energy were performed by taking repeated runs of fixed duration as a function of polarizer angle with the laser tuned and detuned to eliminate the direct electron excitation signal. Four measurements, at polarizer angles separated by 90° to eliminate small instrumental asymmetries, were made for each polarization measurement. Total cross-section measurements were normalized to the electron beam current measured at the Faraday cup.

Experimental conditions were varied to establish sources of systematic error. Three sources were considered: pressure depolarization due to radiation trapping, magnetically induced Hanle effects and optical pumping. Radiation trapping effects were investigated by operating over a range of atom beam pressures. Radiation trapping occurs mainly in the  $6^1\text{S}_0 \rightarrow 6^1\text{P}_1$  transition leading to depolarization of the stepwise signal. At the operating pressures required for a reasonable stepwise fluorescence, depolarizations of about 20% for the  $I = 0$  and 4% for the  $I = \frac{1}{2}$  isotope were observed. Corrections were made by extrapolating back to zero tank pressure, which introduced an estimated uncertainty of 4% and 1.5% in the  $I = 0$  and  $\frac{1}{2}$  polarization data respectively.

Depolarization of the signal due to the Hanle effect arising from residual magnetic fields was investigated by applying a magnetic field parallel to the electron beam direction so as not to deflect the beam. No change in polarization was observed as the magnetic field varied over the range 0–250 mG in the interaction region. The

Helmholtz coils normally provided cancellation of residual magnetic fields within the interaction region to less than 20 mG.

The stepwise signal polarization was measured as a function of input laser power to monitor any optical pumping effects. No change in polarization was observed for the range of laser intensities 5–50 mW mm<sup>-2</sup>.

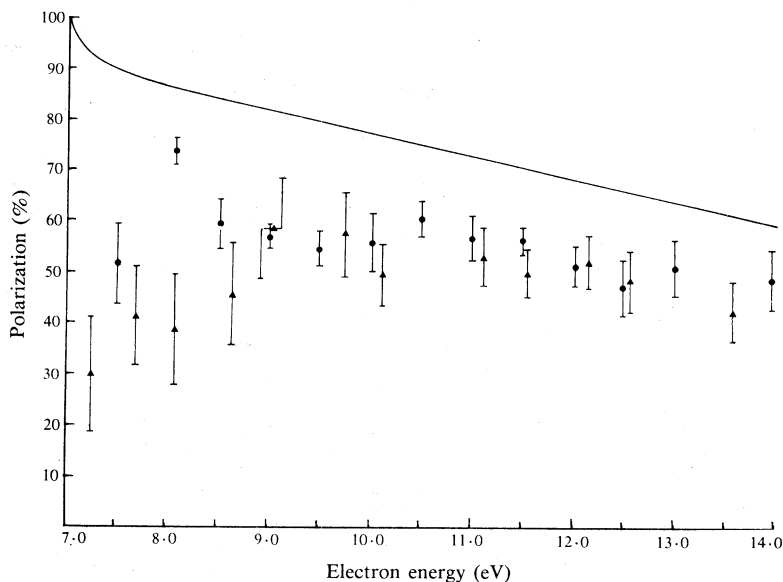


**Fig. 4.** Experimental and theoretical polarization values for the 185 nm line. Experimental uncertainties are 90% confidence limits. Circles are our  $I = 0$  isotope data and triangles the Ottley *et al.* (1974) data for the naturally occurring isotope mixture using direct electron excitation. The solid curve is the theoretical prediction of McConnell and Moiseiwitsch (1968) for the  $I = 0$  isotope.

#### 4. Results and Discussion

To reduce experimental uncertainties, up to twenty individual measurements of the 313 nm line polarizations were taken at a given incident electron energy. The mean and standard deviation of these measurements were determined and used in equation (5) to determine the mean and standard deviation of the ratio of partial total cross sections  $Q_0/Q_1$  for the  $I = 0$  isotopes under circularly polarized laser excitation. These values were then used in equation (6) to determine the line polarization and its standard deviation for the 185 nm line. The polarization obtained was corrected for pressure depolarization by extrapolating back to zero tank pressure and the added uncertainty was incorporated into the experimental uncertainty.

The total excitation cross section  $I(0^\circ) + 2I(90^\circ)$  for the  $I = 0$  isotopes was obtained by using expression (4) for the fluorescence intensity of the 313 nm line:

$$I(185 \text{ nm}) \propto \frac{Q_0/Q_1 + 2}{12(3Q_0/Q_1 + 7)} I(313 \text{ nm}). \tag{11}$$

Substitution into equation (11) of  $Q_0/Q_1$  values determined from the polarization data together with the 313 nm total excitation cross-section data thus gives the 185 nm total excitation cross-section data.

Fig. 4 shows the theoretical and experimental polarization values of the 185 nm line for the  $I = 0$  isotope. Circularly polarized rather than linearly polarized laser excitation was used because it was found both theoretically and experimentally that greater sensitivity is obtained for polarization measurements. The theoretical predictions (solid curve) of McConnell and Moiseiwitsch (1968) used the Coulomb approximation with intermediate coupling wavefunctions to represent the mercury atom. The Ochkur approximation was used to determine the polarization. This theory is not expected to be good for low incident electron energies. The  $I = 0$  experimental data exhibit a decrease in polarization towards threshold in contrast to the theoretical predictions. The experimental results confirm the behaviour near threshold observed by Skinner and Appleyard (1927) and Ottley *et al.* (1974). Comparison with polarization data obtained by Ottley *et al.* (triangles in Fig. 4) for the direct excitation of the naturally occurring isotope mixture, which is dominated by the  $I = 0$  isotopes, is in reasonable agreement with our  $I = 0$  data, except in the vicinity of 8 eV, once allowance is made for the larger experimental uncertainties in their data.

The total excitation cross-section data for the  $I = 0$  isotopes obtained in this work are shown in Fig. 5.

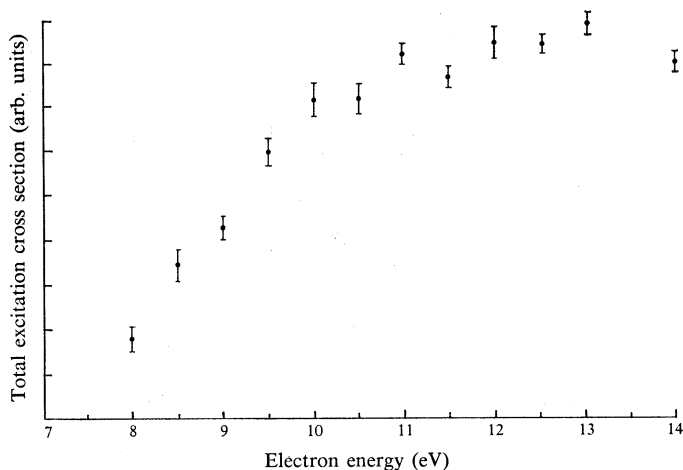


Fig. 5. Total excitation cross-section data for the 185 nm line of the  $I = 0$  isotopes.

### 5. Test of Percival–Seaton Hypothesis

A direct test of the Percival–Seaton hypothesis can be made by comparing the ratios of partial total cross sections  $Q_0/Q_1$  obtained from the  $I = 0$  and  $\frac{1}{2}$  polarization data, using equations (5) and (9) respectively. As mentioned in Section 2, equation (9) depends explicitly on the Percival–Seaton hypothesis. Table 1 shows a comparison of  $Q_0/Q_1$  data. At higher energies the agreement is good, but nearer threshold a marked discrepancy exists which lies well outside the 90% confidence limits for the data, indicating a breakdown in the Percival–Seaton hypothesis at these energies.

Several authors have speculated on the conditions under which a breakdown of the Percival–Seaton hypothesis might occur. Hertel and Stoll (1978) concluded that appropriate conditions could arise if the collision time between the electron and atom was of the same order of magnitude as the inverse of the hyperfine splittings

**Table 1. Ratio of partial total cross sections  $Q_0/Q_1$  for  $I = 0$  and  $\frac{1}{2}$  isotopes**  
 Experimental uncertainties are 90% confidence limits

Electron energy (eV)	$Q_0/Q_1$		Electron energy (eV)	$Q_0/Q_1$	
	$I = 0$	$I = \frac{1}{2}$		$I = 0$	$I = \frac{1}{2}$
8.0	$5.60^{+0.62}_{-0.52}$	$3.05^{+0.42}_{-0.36}$	9.5	$3.38^{+0.34}_{-0.30}$	$3.54^{+0.58}_{-0.45}$
8.5	$3.90^{+0.70}_{-0.54}$	$2.43^{+0.15}_{-0.14}$	10.0	$3.51^{+0.67}_{-0.51}$	$3.52^{+0.66}_{-0.51}$
9.0	$3.64^{+0.26}_{-0.23}$	$3.36^{+0.23}_{-0.21}$	10.5	$4.01^{+0.44}_{-0.37}$	$3.42^{+0.50}_{-0.41}$

of the transition under study, and pointed out that long range interactions could prolong the duration of the collision time. The presence of negative-ion resonances could also prolong the collision time. The observation of a breakdown in the Percival–Seaton hypothesis in mercury is therefore not entirely unexpected because of the strong spin–orbit interactions, which give rise to a large hyperfine structure, and the presence of very strong negative-ion resonances for electron excitation of many states in mercury. The  $6^1P_1$  hyperfine splittings are of the order of 10 GHz and though no high resolution electron excitation studies of the  $6^1P_1$  level have been carried out, our polarization data show evidence of structure at 8 eV which might well be due to resonances. It is also possible that electron–electron correlations (Heideman *et al.* 1980) play a role in the breakdown of the Percival–Seaton hypothesis.

**References**

Bhaskar, N. D., Jaduzliwer, B., and Bederson, B. (1976). *Phys. Rev. Lett.* **38**, 14–17.  
 Blum, K., da Paixão, F. J., and Csanak, G. (1980). *J. Phys. B* **13**, L257–61.  
 Heideman, H. G. M., van de Water, W., and van Moergestel, L. J. M. (1980). *J. Phys. B* **13**, 2801–7.  
 Hertel, I. V., and Stoll, W. (1977). *Adv. Atom. Mol. Phys.* **13**, 113–228.  
 Langendam, P. J. K., Gavrila, M., Kaandorp, J. P. J., and van der Wiel, M. J. (1976). *J. Phys. B* **9**, L453–7.  
 McConnell, J. C., and Moiseiwitsch, B. L. (1968). *J. Phys. B* **1**, 406–13.  
 Macek, J., and Jaecks, D. H. (1971). *Phys. Rev. A* **4**, 2288–99.  
 McLucas, C. W., MacGillivray, W. R., and Standage, M. C. (1982a). *Phys. Rev. Lett.* **48**, 88–92.  
 McLucas, C. W., Wehr, H. J. E., MacGillivray, W. R., and Standage, M. C. (1982b). *J. Phys. B* **15**, 1883–98.  
 Ottley, T. W., Denne, D. R., and Kleinpoppen, H. (1974). *J. Phys. B* **7**, L179–82.  
 Percival, I. C., and Seaton, M. J. (1958). *Phil. Trans. R. Soc. London A* **251**, 113–38.  
 Phillips, M. H., Anderson, L. W., and Lin, C. C. (1981). *Phys. Rev. A* **23**, 2751–3.  
 Register, D. F., Trajmar, S., Jensen, S. W., and Poe, R. T. (1978). *Phys. Rev. Lett.* **41**, 749–52.  
 Schüler, H., and Jones, E. G. (1932). *Z. Phys.* **77**, 801–10.  
 Skinner, H. W. B., and Appleyard, E. T. S. (1927). *Proc. R. Soc. London A* **117**, 224–44.

